This article has been accepted for publication in a future issue of this journal, but has not been fully edited. Content may change prior to final publication.
Citation information: DOI: 10.1109/TCE.2025.3535142, IEEE Transactions on Consumer Electronics

Adaptive Resource Scheduling Algorithm for Multi-Feature Optimization in Personalized Wireless Body Area Networks

Zheng Zhang, *Member, IEEE,* Xinxing Ren, *Student Member, IEEE,* Chun Sing Lai, *Senior Member, IEEE,* Ruiheng Wu, *Senior Member, IEEE,* Jinzhao Lin, and Zhangyong Li

***Abstract*—Wireless Body Area Network (WBANs), as a crucial technology in the field of healthcare monitoring, also plays a significant role in personal consumer electronics (CE). However, existing solutions have yet to effectively address challenges such as personalized demands, data heterogeneity, and dynamic link variations caused by diverse environmental factors. To address these issues, this study proposes a novel approach based on the IEEE 802.15.6 standard, which incorporates personalized node characteristics to cater to individual needs and adapt to node heterogeneity. Furthermore, a dynamic scheduling mechanism for node data is introduced, leveraging multi-feature environmental factors to enhance the practicality of WBAN systems. Finally, for real-time scheduling of emotional anomaly data, this study incorporates skin conductance nodes for the first time to evaluate emotional factors, ensuring the efficient transmission of urgent data. Theoretical analysis and simulation results demonstrate that the proposed approach significantly outperforms traditional methods in terms of energy efficiency, latency, throughput, and resource balance.**

***Index Terms*— Wireless Body Area Networks, Personalized Optimization, Adaptive Resource Management, Dynamic Scheduling.**

I. Introduction

THE significant advancements in the Internet of Things (IoT) have greatly intensified the interaction between the physical and digital realms, permeating various domains and profoundly impacting diverse facets of our daily lives [1], [2]. Wireless Body Area Network (WBANs) as pivotal solutions for precise, personalized, and convenient medical services, have garnered significant attention in the realm of personal consumer electronics (CE) [3]. In recent years, WBANs have been recognized as a critical component of next-generation CE and consumer technologies (CT), particularly in the context of addressing user-specific demands [4]. For instance, WBAN technology is extensively applied in wearable devices, supporting multifunctional CE that integrate health monitoring and entertainment features (e.g., smart-watches and ear-worn devices), personalized fitness tracking systems, electronic health records (EHR), and user-centric smart home systems. These applications not only fulfill the requirements for real-time performance and high reliability but also drive consumer dependency on health and entertainment devices. Furthermore, the research and application of WBANs in CE have evolved from standalone data collection to multi-functional, integrated systems. For example, wearable devices now combine vital sign monitoring, emotion recognition, and health intervention functionalities, while smart home systems leverage WBANs in collaboration with IoT devices to provide personalized and seamless health management experiences. These innovations highlight the potential of WBANs to enhance user experience, optimize energy efficiency, and improve data management, reinforcing their role as a driving force for innovation in the CE industry.

WBAN is specifically designed for human application, utilizing low-power and miniaturized physiological sensors to collect diverse physiological data and individual vital signs, whether located externally or internally on the body [5], [6]. For example, wearable devices, powered by intelligent sensors, enable real-time monitoring and diagnosis of health conditions through smart watches and smartphones. These devices possess the capability to track vital signs such as heart rate, blood pressure, electrocardiogram (ECG), activity levels (including body acceleration and sleep quality), and even audio cues, thereby facilitating effective health management and diagnosis [7], [8]. Depending on the application type, these data are transmitted via a one-hop star topology to a central coordinator (Sink), whereupon reception, they can be forwarded to remote or cloud-based platforms for health monitoring services [9], [10].

In order to meet the diverse quality of service (QoS) requirements of physiological sensors, the IEEE 802.15.6 standard was introduced in 2012 [11], delineating technical requisites such as differentiated QoS, data transmission reliability, and energy efficiency. Various resource scheduling mechanisms have been proposed to optimize these performance metrics. However, existing methods have yet to deeply consider the personalized characteristics stemming from individual bodily

This work was supported in part by the National Natural Science Foundation of China under Grant U21A20447, 62311530103 and 62171073, and in part by the Ph.D. Talent Training Program of Chongqing University of Posts and Telecommunications under Grant BYJS202206. *(Corresponding author: Chun Sing Lai; Zhangyong Li.)*

Zheng Zhang and Jinzhao Lin are with the School of Communications and Information Engineering, Chongqing University of Posts and Telecommunications, Chongqing 400065, China (e-mail: Zheng.Zhang2@brunel.ac.uk; linjz@cqupt.edu.cn).

Zhangyong Li is with the Chongqing Engineering Research Center of Medical Electronics and Information Technology, Chongqing University of Posts and Telecommunications, Chongqing 400065, China (e-mail: lizy@cqupt.edu.cn).

Xinxing Ren, Chun Sing Lai, and Ruiheng Wu are with the College of Engineering, Design and Physical Sciences, Brunel University of London, UB8 3PH, United Kingdom (e-mail: xinxing.ren@brunel.ac.uk; chunsing.lai@brunel.ac.uk; ruiheng.wu@brunel.ac.uk).

Digital Object Identifier xx

differences and data heterogeneity, which are pivotal for catering to personalized demands.

To address this limitation, several algorithms based on multi-factor weighting have been proposed [12]–[21], considering the heterogeneity of different nodes and subjectively weighting various factors to derive final weight factors for sorting. Nevertheless, these multi-factor weighting algorithms inherently rely on subjective weights assigned by decision-makers and fail to objectively reflect real-time environments or adequately consider the differences in individual diseases, while also neglecting the influence of environmental factors on data.

To tackle the scheduling challenges present in real-time environments, some studies have proposed solutions [22]–[30] such as addressing dynamic changes in body posture [22], [23], [25], [26] and introducing temperature-aware routing protocols [30]. However, these methods mostly address singular factors, overlooking individual differences. Furthermore, existing resource scheduling methods [31]–[39] exhibit limitations when dealing with emergency data uploads. While some work focuses on emergency data uploads, accurately determining emergency data remains largely unexplored. Individual emotional factors are also overlooked, as fluctuations in individual emotions may cause data anomalies, thereby affecting the judgment of data uploads.

As a personalized WBAN system, it is imperative to comprehensively consider personalized individuals, node heterogeneity, real-time environmental factors, as well as the determination and upload of emergency data, among other factors. In this paper, we propose a personalized multi-feature adaptive resource allocation algorithm to address the challenges posed by individual bodily differences and data heterogeneity, dynamic changes in real-time environments, such as node temperature variations, and issues arising from data anomalies resulting in emergency data uploads, thereby making the WBAN system more aligned with personalized demands and enhancing overall system performance.

The main contributions of this paper are listed as follows:

- We devised a personalized sorting mechanism to address the resource scheduling requirements of diverse individualized entities and heterogeneous nodes. Compared to existing resource scheduling mechanisms, our proposed mechanism stands out in its integration of improvements to node prioritization based on the IEEE 802.15.6 standard, while considering node heterogeneity and individual disease factors, thereby imbuing the WBAN system with greater personalized characteristics.
- Specifically, we introduce a real-time adaptive scheduling scheme to address various environmental factors, including body tissue damage due to node temperature changes, body posture changes, energy consumption changes, reduced reliability and loss of energy caused by changes in body posture.
- Furthermore, we incorporated emotional factors to monitor whether anomalous data constitutes emergency data, and perform real-time scheduling of emergency data. This contribution, presented for the first time in this paper, which not only ensures the rational scheduling of emergency data and improves network resource utilization but also enhances the practicality of the WBAN system compared to existing resource scheduling solutions.
- To evaluate the performance of the proposed scheduling algorithm, we adhere to the association process and transaction framework outlined in IEEE 802.15.6. This methodology ensures a comprehensive assessment of our simulation results, enhancing the reliability of our experimental research and aligning it closely with real-world scenarios.

The remainder of this paper is organized as follows. Section II summarizes related works on scheduling strategies. The system model is presented and formulated in Section III. Section IV introduces the extraction of personalized factors for adaptive scheduling. The proposed scheduling strategy is described in detail in Section V. Section VI evaluates the performance of the proposed algorithms via simulation. Finally, the paper is concluded in Section VII.

II. Related Work

In this section, we clarify the reasons why the existing resource management mechanisms have difficulty satisfy the personalized WBANs.

A. Multifactor-based Scheduling Strategy

The multifactor-based scheduling strategy comprehensively considers various factors of nodes for prioritization [12]–[21]. The authors [12] proposed a utility function calculation that incorporates factors such as node importance, sampling rate, timeout conditions, and remaining energy to enhance both network service quality and efficiency. The authors [13] designed a link scheduling strategy based on three key factors: medical severity, Age of Information (AoI), and energy consumption. Das et al. [14] calculated the importance of sensor devices based on diverse sensor parameters, achieving certain improvements in energy efficiency, reliability, and reduction of packet loss probability. Wu et al. [15] introduced an energy-efficient data forwarding strategy by taking into account factors such as remaining energy level, sampling frequency, and sensor importance, coupled with data compression to balance sensor energy consumption. In [16] devised a hybrid cost parameter to evaluate the effectiveness of energy efficiency and service quality, minimizing total hybrid cost through optimization of node transmission rate, transmission power, and slot allocation. In [17] dynamically adjusts node transmission order and duration based on channel status and application context to optimize both service quality and energy efficiency. Ullah et al. [18] proposed a perception clustering and cooperative routing protocol, considering factors such as remaining energy, transmission power, communication link signal-to-noise ratio, and total network energy loss for link scheduling. Liang et al. [19] designed a multi-level priority division method based on patient health parameters and data types, employing a tiered slot allocation approach for node data scheduling. Kim et al. [20] proposes a Multi-Criteria Decision Making (MCDM) approach for the link scheduling of node data. Misra et al.

This article has been accepted for publication in a future issue of this journal, but has not been fully edited. Content may change prior to final publication.
Citation information: DOI: 10.1109/TCE.2025.3535142, IEEE Transactions on Consumer Electronics

[21] introduced a slot allocation algorithm considering the importance of health data and the energy consumption rate of transmitting Low-Density Parity-Check Units (LDPU) for node data scheduling.

These approaches consider data heterogeneity and to some extent achieve the goals of reducing energy consumption and enhancing Quality of Service (QoS). However, existing methods have yet to delve deeply into addressing individual bodily differences, and their consideration of real-time environmental factors is not comprehensive.

B. Environmental Factor-Aware Scheduling Strategy

Environmental factor-aware scheduling strategy primarily focus on adapting data transmission in response to variations in environmental conditions [22]–[30]. The author [22] proposed a cross-layer energy-aware resource allocation scheme that improves system performance by considering both link quality and transmission power. The author [23] introduced a link quality-aware resource allocation scheme in WBAN, which consists of two phases: temporal link quality measurement and subchannel allocation among WBANs, aiming to maximize the overall network performance. In [24] presented a transmission rate-adaptive energy-saving resource allocation scheme that takes into account the dynamic characteristics of links and node transmission rates. In [25] addressed the improvement of system service quality by considering sensor requirements for channel quality and packet error rate. Selem et al. [26] introduced the ”mobTHE” protocol to address sensor node mobility issues. Mao et al. [27] optimized WBAN energy efficiency by considering path loss and shadowing values of different nodes. Zhang et al. [28] used the Particle Swarm Optimization (PSO) algorithm to optimize the total cost of delay and energy consumption under posture state. In [29] considered a closed-loop control mechanism alongside a hybrid operation of posture and motion detection, using body communication RSSI values to approximate signal attenuation within a user’s gait cycle, and using acceleration signals to determine position within the gait cycle, thereby reducing energy consumption. In [30] proposed a TLD-RP perception routing protocol that takes into account temperature, link reliability, and latency to meet QoS requirements. While these methods address data transmission issues arising from environmental variations, they overlook individual differences within WBANs.

C. Anomalous Data Detection Resource Scheduling Strategy

The resource scheduling strategy for anomalous data detection involves emergency resource allocation by redesigning superframes and relay transmission methods [31]–[39]. In [31] proposed a low-power Medium Access Control (MAC) protocol that detects and handles emergencies within the body sensors by modifying the superframe structure and allocating priorities. In [32] designed an emergency priority slot allocation scheme that uses relay nodes for channel detection and processing of emergency data. The author [33] introduced a stochastic graph-inspired Deep Deterministic Policy Gradient (DDPG) algorithm and transforms the problem into a Markov decision process to ensure the reliability and energy efficiency of emergency critical physiological data transmission. The author [34] proposed a channel access scheme for nodes carrying emergency data frames to improve the reliability of emergency data frame transmission. Olatinwo et al. [35], [36] proposes a Coordinated Superframe Duty Cycle Hybrid MAC (SDC-HYMAC) protocol and a Multi-Channel Hybrid Medium Access Control (MC-HYMAC) protocol to ensure the latency and energy efficiency of emergency critical physiological data transmission. Manirabona et al. [37] presented a Priority Weighted Round Robin (PWRR) scheduling strategy to support QoS for emergency traffic. The algorithm combines priority scheduling and weighted RR, using user priorities of physiological data to determine how to schedule and transmit them to the WBAN. Misra et al. [38] addressed the scheduling of emergency data by adjusting the data rates of different nodes and using priority adjustments. Moulik et al. [39] proposed an Adaptive-Toggle MAC (AT-MAC) activation algorithm that adjusts the MAC frame payload of WBAN sensor nodes conforming to the IEEE 802.15.4 protocol based on the severity of health parameters measured by each sensor node. These methods facilitate emergency transmission of anomalous data; however, they fail to consider fluctuations in individual emotions, and anomalous data may not necessarily be urgent, potentially leading to a decline in overall network resource efficiency.

Our work provides a comprehensive synthesis of the aforementioned efforts. Firstly, we consider both node heterogeneity and individual personalization, enhancing the adaptability of the system to diverse user profiles. Secondly, we address real-time variations induced by environmental factors. Thirdly, we incorporate emotional factors in anomaly detection for data assessment. These aspects collectively aim to tackle existing challenges, thereby striving towards the development of a more personalized and practical WBAN system.

III. System Model

In this section, we will describe the network model based on IEEE 802.15.6 standard, detailing the establishment of connections between Sink and sensing nodes, and expounding on the beacon mode with superframes structure.

A. Network Model

Consider a typical WBAN system based on the IEEE 802.15.6 standard, comprising a Sink and n sensing nodes, as illustrated in Fig. 1. The Sink and sensing nodes are interconnected in a one-hop star topology. Each sensing node collects distinct physiological data and forwards it to the Sink based on specific time slots (for example, a pulse oximeter measures blood oxygen saturation levels and heart rate, an electrocardiogram sensing monitors and records a patient’s electrocardiogram). Sensing nodes perceive health parameters as continuous functions of time and transmit them to the Sink. We employ a beacon-based superframe structure as the access mode, wherein the hub broadcasts beacon frames at each beacon cycle scenario. Table I presents the significant physiological parameters monitorable by WBAN [40]. During the connection establishment process, the Sink, based on

This article has been accepted for publication in a future issue of this journal, but has not been fully edited. Content may change prior to final publication.
Citation information: DOI: 10.1109/TCE.2025.3535142, IEEE Transactions on Consumer Electronics

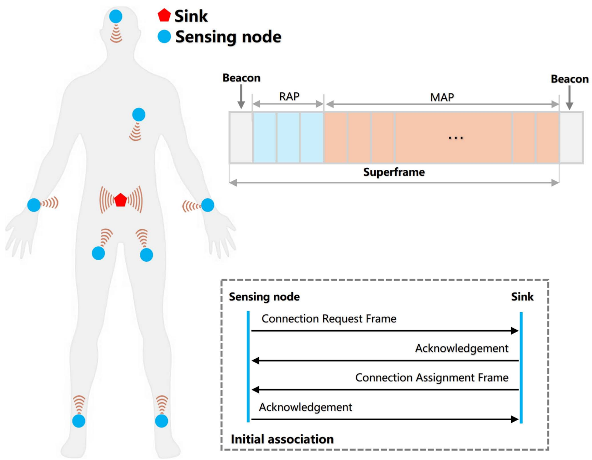

Fig. 1. Illustration of a WBAN system.

TABLE I
DIFFERENT TYPES OF MEDICAL SENSORS

Sensing type	Data rate	Bandwidth	Modified priority
EMG	320 kbps	0-10000 Hz	1
ECG	288 kbps	100-1000 Hz	1
EEG	42.3 kbps	0-150 Hz	2
Glucose	1600 bps	0-50 Hz	2
Temperature	120 bps	0-1 Hz	3
Cochlear implant	100 kbps	-	3
Voice	50-100 kbps	-	4

interaction information, discerns which sensing nodes need to transmit data and determines the transmission sequence of these sensing nodes.

B. Association Establish and Superframe Structure

The superframe structure consists of a beacon, a random access phase (RAP), and a management access phase (MAP), as shown in Fig. 1. To accommodate different types of data, the beacon is transmitted first in each superframe to establish connections with sensing nodes. During the RAP phase, sensing nodes obtain access to channels through fair contention mechanisms for handling various traffic types. The MAP phase is used to schedule the uplink and downlink allocation intervals. To obtain the allocation intervals for uplink scheduling in MAP, an association between sensing nodes and the Sink is required. The Sink initiates by broadcasting beacon frames, and unassociated nodes, upon receiving the beacon frames, use carrier sense multiple access with collision avoidance (CSMA/CA) to transmit connection request frames during the RAP. The connection request frames contain link request information element (IE) fields, where the IE element ID field identifies the type of connection request, and the Length and allocation request fields specify the total bytes of the allocation request. To request uplink allocation intervals in the MAP, sensing nodes must specify the number of slots that can meet the QoS requirements in the allocation request field. To approve the uplink allocation requests, the Sink must send link allocation frames containing link allocation IEs. To initialize the link allocation IEs, the Sink need to sequentially approve the received uplink allocation requests based on the initial link scheduling algorithm.

IV. PERSONALIZED FACTOR EXTRACTION FOR ADAPTIVE SCHEDULING

The primary objective of this study is to provide WBAN systems with personalized features and environmental factors that are better aligned with practical scenarios, while also enabling the identification and real-time transmission of anomalous data. To achieve this goal, the chapter elaborates on the explanatory and design aspects of the feature variables in the proposed scheduling algorithms.

A. Personalized Feature Design

The heterogeneous nature of sensor nodes in WBANs poses significant challenges for system design and scheduling. This heterogeneity arises from differences in computational capabilities, storage capacities, and energy resources among nodes, as well as variations in the type and urgency of data generated based on each node's functional role. To address these challenges, we developed key node features, including enhanced node priority, personalized disease-related functionalities, and variations in data packet lengths driven by differences in sampling rates. These features enable optimized resource allocation and scheduling strategies, improving overall system performance.

1) Prioritization Improvements Based on IEEE 802.15.6 Standard: Although IEEE 802.15.6 standard provides eight levels of priority classification for nodes, it fails to adequately reflect the heterogeneous data requirements. The multitude of priority levels not only fails to accurately capture the significance of node data but also may impede transmission efficiency. Moreover, critical data types such as EMG, ECG, etc., cannot be simply distinguished based on priority levels alone. Furthermore, individual WBAN users may exhibit varying priority requirements for nodes. Thus, building upon the standard classification, we propose a rational categorization of node priorities during the initial phase.

$$\phi_i = \lceil \frac{p_i}{2} \rceil \tag{1}$$

where p_i represents the eight original priority levels defined in the IEEE 802.15.6 standard, and ϕ_i denotes the refined priorities.

2) Feature Design Based on Individual Disease: Due to the presence of different individual diseases within each WBAN entity, the physiological data generated by individual nodes possess varying degrees of importance. For instance, data on heart rate produced by individuals with cardiac conditions should be considered more critical compared to those generated by individuals without such conditions. In addition, in some cases, anomalies in blood glucose levels from diabetic individuals with normal heart function may even take precedence over anomalies related to heart conditions. Therefore, we have established disease-specific feature parameters as follows:

$$\varrho_i = \begin{cases} 1, & Disease\ related \\ 0, & Disease\ unrelated \end{cases} \tag{2}$$

This article has been accepted for publication in a future issue of this journal, but has not been fully edited. Content may change prior to final publication.
Citation information: DOI: 10.1109/TCE.2025.3535142, IEEE Transactions on Consumer Electronics

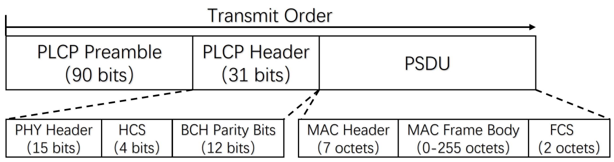

Fig. 2. Frame format of the IEEE 802.15.6 standard.

where ϱ_i is determined to be pertinent to patients based on bodily characteristics.

3) Feature Design Based on Data Length: The data streams generated by different sensing nodes exhibit diverse traffic patterns, including continuous or periodic data transmissions, or transmissions triggered by sudden events (such as a cardiac event). Therefore, the Sink must allocate slots that precisely match the traffic generation times of each node to avoid delays or bandwidth wastage. Additionally, accurate calculation of the round-trip time required for data transmission, as well as the physical layer (PHY) characteristics and data length, is essential, as illustrated in Fig. 2.

The calculation formula is provided as follows:

$$T_F(L_p, mode) = t_{pre} + t_{PLCP_{header}} + t_F(L_p, R_{mode}) \quad (3)$$

the first part is given by $t_{pre} = \frac{N_{pre}}{R_s}$, the second part by $t_{PLCP_{header}} = \frac{N_{header} \cdot S_{PLCP_{header}}}{R_s}$, and the third part by $t_F(L_p, R_{mode}) = \frac{N_{total}}{\log_2 M \cdot R_s}$, where N_{pre}, N_{header}, and S_{header} represent the length of the preamble, physical layer convergence protocol (PLCP) header, and PLCP service data unit (PSDU), respectively. R_s and M are the symbol rate and cardinality of the constellation of a given modulation scheme, respectively. Furthermore, $S_{PLCP_{header}}$ and N_{total} respectively refer to the spreading factor of the PLCP header and PSDU.

To facilitate transmission, each node should request the required number of slots upon initiating association with the Sink. The length of the allocated slots requested by the node is defined as $pASlotMin + L_p \times pASlotRes$, the calculation for the requested allocation slots is as follows:

$$L_p = \frac{T_F(L_p, mode)}{pASlotRes} \quad (4)$$

where $pASlotMin$ and $pASlotRes$ are set to 500 microseconds.

B. Environmental Feature Design

Moreover, environmental features further exacerbate this heterogeneity. Defined environmental factors include variations in node temperature, changes in body posture, and fluctuations in personal emotions. To adapt to these dynamic conditions, we introduced a flexible scheduling mechanism that adjusts node operations based on real-time monitoring data, thereby enhancing the robustness and reliability of WBAN systems under complex scenarios.

TABLE II
PARAMETERS OF PENNER BIOHEAT MODEL

Parameter	Value
ρ	50 kg/m^3
C	20.94 J/(kg·K)
k	0.5 W/(m·°C)
Q	9.05 W/m^3

TABLE III
INITIAL RELATIVE DISTANCE BETWEEN SINK AND NODES

Posture Type	Standing	Walking
EEG (Head)	38 cm	38 cm
ECG (Left Upper-chest)	15 cm	15 cm
Glucose (Left Lower-torso)	13 cm	13 cm
Insulin Pump (Right Lower-torso)	12 cm	12 cm
Blood Pressure (Left Arm)	15 cm	30 cm
SPO2 (Right Arm)	14 cm	31 cm
EMC (Left Leg)	58 cm	67 cm
Temperature (Right Leg)	57 cm	64 cm
Skin Conductance (Center of Torso)	0 cm	0 cm

1) Feature Design Based on Node Temperature: The frequent interaction of information between Sink and sensing nodes generates a significant amount of radio frequency (RF) energy, which may cause an increase in body temperature and damage to body tissues. Particularly, the heat generated by nodes implanted in skin tissue may lead to a burning sensation and discomfort, with the potential for tissue damage in areas with low blood flow. We introduce the Penner bioheat equation to assess body temperature, as shown:

$$\rho C \frac{\partial T}{\partial t} = \nabla \cdot (k \nabla T) + Q_b + Q \quad (5)$$

where ρ is tissue density (kg/m^3), C is the specific heat (J/(kg·K)), k is the thermal conductivity (W/(m·°C)), T is temperature (°C), and Q is the microwave power density (W/m^3). In the heat conduction process, the symbol ∇ indicates the gradient operation on the temperature field T, yielding the spatial rate of change of temperature. $\nabla \cdot (k \nabla T)$ represents the divergence operation on the heat conduction flux, describing the loss or accumulation of heat in space. Q_b is a term accounting for perfusion effects, defined as follows:

$$Q_b = \rho_b w_b C_b (T - T_a) \cdot \rho \text{SAR} \quad (6)$$

where SAR represents the specific absorption rate, which quantifies the rate at which body tissues absorb energy when exposed to RF radiation, and can be expressed as SAR $= \frac{\sigma |E|^2}{\rho}$. E denotes the induced electric field, σ is the electrical conductivity, ρ_b is the blood mass density (kg/m^3), w_b is the blood perfusion rate (1/s), C_b is the blood specific heat (W/(m·°C)), and T_a is the ambient blood temperature (°C) before entering the ablation region (relevant parameter values detailed in Table II [41].

2) Feature Design Based on Body Posture: In WBAN systems, individual posture changes and body movements lead to variations in network topology, consequently causing channel fading. This results in degraded network performance, including increased energy consumption, decreased

This article has been accepted for publication in a future issue of this journal, but has not been fully edited. Content may change prior to final publication.
Citation information: DOI: 10.1109/TCE.2025.3535142, IEEE Transactions on Consumer Electronics

TABLE IV
PARAMETERS OF PATH LOSS MODEL

Parameter	Value
d_0	50 mm
$PL(d_0)$	20.94 dB
n	4.99 dB
S	9.05 dB

throughput, and elevated packet error rate, among others. By integrating mobility and propagation models and considering posture characteristics (the deterministic information provided by each change, i.e., position, orientation, velocity), we utilize the relative distance between the Sink and nodes as a reference model, detailed in Table III [42]. It is important to note that the effective communication range between the Sink and nodes is limited to within 2 meters.

Additionally, based on the predetermined values provided in Table IV [42], we calculate the average channel gain (in dB). After estimating the RX power using propagation loss models, we obtain the received signal strength (RSS) and corresponding signal-to-interference-plus-noise ratio (SINR) for transmission evaluation. Specifically, SINR and physical layer (PHY) transmission parameters are used to determine the bit error rate (BER) and packet error rate (PER) between nodes and the Sink.

$$PL(d) = PL(d_0) + 10n \cdot log_{10}(d/d_0) + S \tag{7}$$

where d is the distance between the node and the Sink. Additionally, $PL(d_0)$ represents the path loss at a reference distance d_0, while n is the path loss exponent. Moreover, S is the body shadow factor.

$$BER_{ij} = \begin{cases} \frac{1}{2} \times e^{-Eb/No}, & DBPSK \\ Q(\sqrt{4^{Eb/No}} \times \sin\left(\sqrt{2} \times \pi/4\right)\right), & DQPSK \end{cases} \tag{8}$$

where Eb/No[dB] denotes the energy per bit-to-noise power spectral density ratio in dBm, is calculated based on the current signal to interference plus Noise ratio (SINR) level as:

$$Eb/No[\text{dB}] = SINR_{ij}^{t}[\text{dB}] + 10 \times \log_{10}(BW/R) \tag{9}$$

where BW represents the bandwidth in Hz and R is the data rate in bps. Furthermore, the packet error rate (PER) between the transmitting node and the receiving node can be assessed as:

$$PER_{ij} = 1 - \left(1 - BER_{ij}^{t}\right)^{n} \tag{10}$$

where n denotes the packet length in bits, and BER is the corresponding bit error rate.

3) Feature Design Based on Personal motions: Different individuals experience varying emotional fluctuations in different scenarios, which can transiently manifest as data anomalies. However, not all anomalous data points signify urgent events. For instance, an increase in heart rate due to heightened anxiety may not necessarily indicate an emergency. Therefore, it becomes essential to discern whether anomalous data should be classified as urgent by introducing skin conductance activity nodes for such determination. Specifically, when abnormal data is detected, the proposed mechanism will obtain the readings of the skin conductance activity node in real time. Since emotional reactions usually show instantaneous and reversible changes in skin conductance, which are usually related to external stimuli or psychological factors, and medical emergencies (such as hypoglycemia or arrhythmia, etc.) are usually manifested as continuous and abnormal changes in skin conductance, and are usually accompanied by abnormalities in other physiological signals. Therefore, we combine auxiliary context-aware parameters (such as heart rate, body temperature, and activity level) and set a threshold based on the individual personalized baseline. If the threshold is exceeded, the skin conductance activity node at this time is set to 1, indicating that the skin conductance node signal has increased significantly, and it is considered to be an abnormality caused by emotional fluctuations; otherwise, the skin conductance activity node is set to 0, and it is considered to be a data abnormality caused by emergency data.

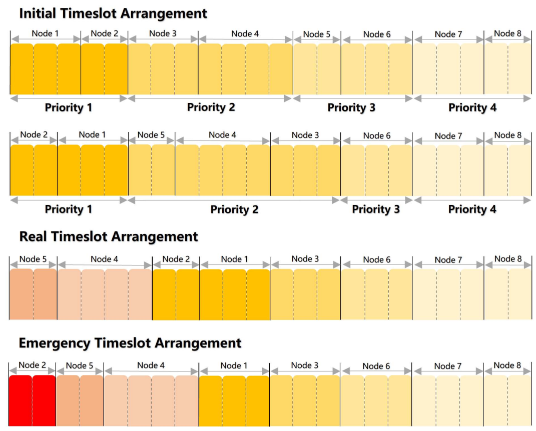

Fig. 3. Optimization process for scheduling startegy.

$$\delta(t) = \begin{cases} 1, & Skin\ conductance\ activity \\ 0, & Skin\ conductance\ unactivity \end{cases} \tag{11}$$

where $\delta(t)$ is utilized for urgent evaluation of abnormal data in skin conductance activity.

The potential risks of false positives or false negatives caused by external factors, such as extreme environmental conditions or sensor noise, will be investigated in future research.

V. PERSONALIZED DYNAMIC LINK SCHEDULING ALGORITHM

In this section, we introduce a personalized dynamic link scheduling algorithm, which is designed to optimize data transmission efficiency in WBAN systems. The algorithm comprises three phases: Initial sorting based on personalized features, real-time environment-based dynamic scheduling, and emergency scheduling for anomalies. These phases work collaboratively to prioritize data transmission according to node characteristics, environmental factors, and emergency conditions, ensuring robustness and adaptability. It is worth noting that the proposed algorithm is inherently adaptable, allowing it to handle scenarios under the homogeneous node

This article has been accepted for publication in a future issue of this journal, but has not been fully edited. Content may change prior to final publication.
Citation information: DOI: 10.1109/TCE.2025.3535142, IEEE Transactions on Consumer Electronics

assumption, treating it as a special case of the general heterogeneous framework.

A. Initial Sorting Based on Personalized Features

In the initial phase, the coordinator extracts personalized characteristics of the nodes, including enhanced high-priority nodes, personalized disease-related nodes, and data length, from the connection request frames. Based on this information, time slots are allocated to minimize unnecessary communication and reduce the energy consumption of low-priority nodes during critical operations. The Information Element (IE) field within the connection request frame contains the number of requested time slots for each node (as described in Section IV. A. 3). Once the features are extracted, the coordinator returns a connection acknowledgment frame. It is important to note that each time slot is set to a duration of 1 ms.

As illustrated in Fig. 3, the goal of the initial scheduling process is to arrange heterogeneous nodes in the uplink allocation interval of the MAP based on their personalized priority levels. Specifically, nodes are first sorted according to the improved four-level priority system. For nodes with specific disease characteristics, their priority is elevated by one level. For example, in the case of the eight nodes shown in Fig. 3, Node 5, initially assigned to priority level 3, is promoted to priority level 2 due to its disease-related characteristics. Additionally, within the same priority level, nodes with disease-related characteristics are given precedence over those without. For instance, the order of Node 1 and Node 2 (priority level 1), as well as Node 3 and Node 4 (priority level 2), is adjusted based on their disease attributes.

The detailed implementation is presented in Algorithm 1. Lines 1 to 3 describe the extraction of node features and the initial sorting based on the enhanced priority levels. Lines 4 to 14 handle the reordering of nodes with disease-related characteristics. Finally, lines 15 to 16 output the final sorted result.

Algorithm 1 Initial Scheduling Based on Personality Nodes Algorithm

Initialization:
CRF_i: Connection Request Frame of node i
D_i: Disease status of node i
Algorithm:
1: **Upon receiving** CRF_i **from node** i
2: Extract personalized features of node i from CRF_i
3: Initialize priority level ϕ_i based on disease characteristics
4: **for** $i \leftarrow 1$ **to** N **do**
5:     **for** $j \leftarrow i+1$ **to** N **do**
6:         **if** $D_i \neq D_j$ **then**
7:             **if** $D_i \neq$ No Disease **and** $D_j =$ No Disease **then**
8:                 $\phi_i \leftarrow \phi_i + 1$
9:             **else if** $D_j \neq$ No Disease **and** $D_i =$ No Disease **then**
10:                 $\phi_j \leftarrow \phi_j + 1$
11:             **end if**
12:         **end if**
13:     **end for**
14: **end for**
15: Sort nodes based on ϕ_i in descending order
16: Transmit data in sorted order

B. Real Time Environment-based Dynamic Scheduling

In real-time data transmission scenarios, the environmental characteristics of nodes play a critical role in resource scheduling and optimization. To quantify and integrate these characteristics effectively, we developed an indicator system based on the Analytic Hierarchy Process (AHP), incorporating three key parameters: (1) Posture and Path Loss-Induced Packet Error Rate (P), which evaluates the communication reliability of nodes under conditions of motion or signal interference; (2) Temperature Variation (T), which reflects the stability of the node's operating environment and its impact on device performance; and (3) Remaining Battery Life (B), which assesses the sustainability of node operation over extended periods. These parameters collectively provide a comprehensive framework for understanding and addressing the dynamic environmental factors affecting real-time data transmission.

The scheduling process utilizes the AHP framework to construct a relative importance matrix for indicators and compute weighted values. The steps are as follows:

1) **Construction and Normalization of the Pairwise Comparison Matrix**: A pairwise comparison matrix x_{ij} is constructed for environmental metrics such as P, T, and B. The matrix is normalized as follows:

$$\bar{x}_{ij} = \frac{x_{ij}}{\sum_n x_{ij}} \tag{12}$$

Here, x_{ij} represents the comparison value for row i and column j, normalized across all metrics.

2) **Calculation of the Feature Vector**: Based on the normalized matrix, the feature vector for each metric is computed as follows:

$$v_i = \frac{\sum_{j=1}^{n} \bar{x}_{ij}}{n} \tag{13}$$

The feature vector v_i represents the relative importance weight of each metric.

3) **Normalization of Real-Time Environmental Features**: Real-time environmental feature values are normalized using a min-max normalization method as follows:

$$y_{ij} = \frac{y_{ij} - \min(y_{ij})}{\max(y_{ij}) - \min(y_{ij})} \tag{14}$$

Here, y_{ij} represents the normalized value of the real-time metric for row i and column j.

4) **Weighted Normalized Value Calculation**: By combining the AHP-derived weights v_i, the weighted normalized values are computed as follows:

$$w_i = \sum_{j=1}^{n} y_{ij} \cdot v_i \tag{15}$$

Citation information: DOI: 10.1109/TCE.2025.3535142, IEEE Transactions on Consumer Electronics

The value w_i reflects the real-time importance of each node. Nodes are dynamically rescheduled based on their w_i values, ensuring efficient allocation of resources.

If a pairwise comparison matrix is defined as shown below, x_{ij} represents the relative importance of factor i to j. This matrix is determined by the Sink node, who evaluates the relative importance of criteria based on network conditions.

$$x_{ij} = \begin{array}{c} \\ \mathrm{P} \\ \mathrm{T} \\ \mathrm{B} \end{array} \!\! \begin{array}{c} \begin{array}{ccc} \mathrm{P} & \mathrm{T} & \mathrm{B} \end{array} \\ \begin{pmatrix} 1 & 2 & 3 \\ 1/2 & 1 & 2 \\ 1/3 & 1/2 & 1 \end{pmatrix} \end{array} \tag{16}$$

After defining the pairwise comparison matrix, the priority vector, represented as the normalized eigenvector of the matrix, is calculated to determine the relative importance of the evaluation criteria. The calculation involves two steps: first, the pairwise comparison matrix is normalized using Equation (12); second, the eigenvector for each criterion i is derived using Equation (13), where v_i denotes the relative priority of i among the criteria. The resulting priority vector is:

$$\begin{array}{c} \\ \mathrm{P} \\ \mathrm{T} \\ \mathrm{B} \end{array} \!\! \begin{array}{c} Result \\ \begin{pmatrix} 0.16 \\ 0.251 \\ 0.589 \end{pmatrix} \end{array} \tag{17}$$

This indicates that criterion B (e.g., battery level) holds the highest weight among the evaluation criteria, while P (e.g., packet error rate) has the lowest weight. Once the priority weights are established, the final scores for each node are calculated by integrating the parameter values for all criteria. This is achieved using the min-max normalization method defined in Equation (14) and the weighted sum equation in Equation (15). Based on the total weighted normalized scores, nodes are scheduled dynamically, ensuring efficient resource allocation that aligns with the relative priorities of the evaluation criteria.

Algorithm 2 implements the scheduling principles through a structured process. First, the weights of all nodes are initialized (Lines 1–3). For nodes belonging to priority level 1, scheduling is determined based on the values of $w_i \times P_4$, with higher values receiving time slots first. For priority level 2 nodes, their $w_i \times P_3$ values are compared with the $w_i \times P_4$ values of priority level 1 nodes, ensuring that nodes with higher comparative values are prioritized for transmission. Similarly, for nodes in priority levels 3 and 4, their respective weights are calculated and sequentially compared following the same principle. The algorithm iterates through all nodes, computes the final order, and returns the resulting schedule S (Lines 4–23).

Algorithm 2 Real-time Dynamic Link Scheduling

Input: List of nodes N, packet error rate PER, temperature of nodes T, battery level of nodes B, priority weight factors P_1, P_2, P_3, P_4.

Output: Scheduling queue S.

```
1: Initialization:
2: Th_PER, Th_T, Th_E: Thresholds for each parameter
3: W: Weighted normalization value
4: Scheduling:
5: Initialize empty queue S
6: for each node n in N do
7:     Calculate w_i for node n
8:     if node priority is 1 then
9:         Compare w_i × P_4 with other nodes' w_i values
10:        Sort node n accordingly
11:    else if node priority is 2 then
12:        Compare w_i × P_3 with other nodes' w_i × P_4 values
13:        Sort node n accordingly
14:    else if node priority is 3 then
15:        Compare w_i × P_2 with other nodes' w_i × P_3 values
16:        Sort node n accordingly
17:    else
18:        Compare w_i with other nodes' w_i values
19:        Sort node n accordingly
20:    end if
21:        Add node n to S
22: end for
23: return S
```

C. Emergency Scheduling for Anomalies

Accurate anomaly detection and classification are critical to distinguish between anomalies caused by emotional fluctuations and those arising from physiological emergencies in WBANs. This distinction ensures that emergency data is prioritized for timely transmission, while avoiding unnecessary resource allocation to non-critical anomalies. To achieve this, we introduce a skin conductance node signal (as described in Section IV. B. 3) to aid in classification. When data anomalies are detected and the skin conductance node signal increases significantly, the anomaly is attributed to emotional fluctuations. Conversely, if the data remains abnormal without a significant increase in the skin conductance signal, it is classified as emergency data. To further enhance anomaly detection accuracy, the sequential probability ratio test (SPRT) is employed. This statistical method detects anomalies in real-time by analyzing deviations in the observed data sequence. The approach dynamically adjusts sensitivity based on system requirements, making it suitable for heterogeneous and dynamic WBAN environments.

Given $X_j = \{x_1, x_2, \ldots, x_n\}$, we calculate the cumulative sum (CUSUM) of negative deviations and positive deviations from the mean, where the positive sum and the negative sum are respectively represented as $S_i^+ = \max\left(0, S_{i-1}^+ + x_i - \overline{x} - \alpha\right);\quad S_0^+ = 0$ and $S_i^- = \min\left(0, S_{i-1}^- + x_i - \overline{x} - \alpha\right);\quad S_0^- = 0$ represents the i-th data in the observed data sequence, $\overline{x}$ denotes the historical mean, and α denotes the shift size, usually set to half of the sample standard deviation. H is referred to as the decision value, usually set to 4 or 5 times the sample standard deviation. In this way, we can adjust the sensitivity of anomaly detection by adjusting α and H. Additionally, if the length of the data set $X_j = \{x_1, x_2, \ldots, x_n\}$ exceeds the maximum size, the oldest data in X_j is deleted, and the new data is added to X_j. After determining the emergency data, the Sink takes measures to

This article has been accepted for publication in a future issue of this journal, but has not been fully edited. Content may change prior to final publication.
Citation information: DOI: 10.1109/TCE.2025.3535142, IEEE Transactions on Consumer Electronics

Algorithm 3 Emergency Data Scheduling Algorithm for Isolated Emotions

Input:
S_c: Skin conductance signal **S**
X_i: Set of observed data for node i
Output:
S_N: Sorted list of nodes
Algorithm:

Initialization:
  $S_N \leftarrow []$ ▷ Initialize list to store sorted nodes
upon receiving data x **from node** i:
  $r \leftarrow \text{CUSUM}(X_i, x)$ ▷ return the result of anomaly detection
if r is true **then**
  if $S_c > \delta$ **then**
    Call Algorithm 2
    if $S_c \leq \delta$ **then**
      if N_{X_i} = 1 **then**
        Sort N_{X_i} and append to S_N
      else if $N_{X_i} > 1$ **then**
        Sort N_{X_i} according to Algorithm 2 and append to S_N
      end if
    end if
  else
    /* Nothing happened */
    Insert x **to** X_i
      Maintain sorting according to Algorithm 2
  end if

prioritize the nodes that generate emergency data to the highest priority level and prioritizes their transmission.

The algorithm first detects anomalies in data using the CUSUM method. Based on the skin conductance signal, anomalies are classified as either emotional or emergency. Emergency data nodes are sorted and prioritized for transmission, while emotional anomalies invoke additional processing. Nodes with no anomalies are maintained in sorted order for efficient scheduling. The specific algorithm is shown in Algorithm 3.

D. Computational Complexity and Resource Requirements Analysis

The proposed algorithm comprises multiple scheduling phases and real-time adjustments, which could raise concerns about computational complexity and resource consumption, particularly for WBAN nodes with constrained processing power and memory. To address this, we conducted a detailed theoretical analysis evaluation of the computational complexity and resource requirements. The analysis was performed using a representative processor, such as the ARM Cortex-M4, which is commonly employed in WBAN devices due to its low power consumption and sufficient computational capabilities.

1) Computational Complexity: For Algorithm 1, the primary operation involves prioritizing N nodes based on their characteristics, achieved through sorting. When using a quicksort-based implementation, the algorithm achieves an average time complexity of $O(N \log N)$. Assuming an average of 20 instructions per comparison and exchange, the total instruction count can be approximated as $20 \cdot N \log_2(N)$. For $N = 50$, the execution time on an ARM Cortex-M4 processor operating at 80 MHz (executing $80 \cdot 10^6$ instructions per second) is approximately 0.07 ms. Algorithm 2 involves recalculating weights and reordering nodes dynamically based on environmental conditions. This process has a time complexity of $O(N^2)$ due to the need for pairwise comparisons among nodes. With an estimated 10 instructions per weight calculation and 5 instructions per comparison, the total instruction count is approximated as $10 \cdot N + 5 \cdot N^2$. For $N = 50$, the execution time is approximately 0.16 ms on the same processor. Algorithm 3 performs anomaly detection via the CUSUM method and sorts nodes based on emergency priorities. The complexity primarily depends on the number of anomalous nodes (M) and scheduled nodes (K). The CUSUM operation has a complexity of $O(M)$, while sorting incurs $O(K \log K)$. Assuming 5 instructions per CUSUM calculation and 20 instructions per sorting operation, the execution time for $M = 10$ and $K = 10$ is approximately 0.01 ms.

2) Resource Requirements: The packet size, which varies based on specific application scenarios, typically ranges from 100 to 2000 bytes (approximately 800 to 16000 bits). Queues are utilized for storing pending data and scheduling tasks, with their size determined by the number of nodes and real-time scheduling requirements. In our implementation, each node maintains a fixed-size priority queue. Assuming 50 nodes, each with a queue length of 10, the total queue capacity is 500 scheduling items. Each queue element (including node ID, priority, and scheduling time) occupies about 64 bits (8 bytes), requiring around 4 KB of memory to store all queue data. In addition to queues, basic node information (e.g., health status, temperature, and priority) and the scheduling algorithm's state must also be stored. Assuming each node's information occupies 64 bits (8 bytes), the storage required for 50 nodes amounts to 400 bytes. The algorithm further requires storage for the sorted node list and intermediate calculation results. Overall, the total memory requirement is estimated to range between 1 KB and 4 KB, depending on the network scale and data volume.

Overall, the algorithm executes in under 1 ms and requires less than 4 KB of memory, making it highly compatible with the resource constraints of modern WBAN nodes. By utilizing fixed-size buffers and priority queues, memory usage is optimized, avoiding the need for extensive data storage. As a result, the algorithm effectively adheres to the memory and processing constraints of WBAN nodes, ensuring its suitability for practical deployment.

VI. Performance Evaluation

In this study, the proposed scheme is sumulated using Python 3.8.2. The computational system comprises a Windows 10 operation system, an Intel Core i7-10700 CPU, and 32GB of RAM.

TABLE V
COMMON SIMULATION PARAMETERS

Parameter	Value
Frequency band	868MHz
Modulation	ASK
Data rate	250 Kbps
Default transmission power	-5dBm
Reception sensitivity	-82 dBm
Channel access mechanism	TDMA
Access mode	Beacon with superframes
Beacon period	255ms
Packet size	50-250 bytes
ACK policy	I-ACK
Sensing duration	50 $\times 10^{-3} ms$
Voltage	2.7 v
Idle/ TX/ RX/ Sleep current	0.4 mA/ 17.4 mA/ 19.7 mA/ 0.03 μA

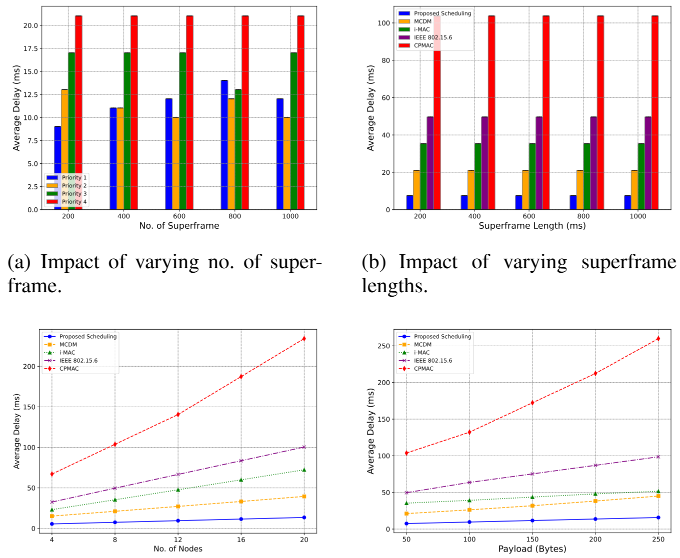

(a) Impact of varying no. of superframe.

(b) Impact of varying superframe lengths.

(c) Impact of varying no. of nodes.

(d) Impact of varying payload.

Fig. 4. Comparison of average delay.

A. Simulation Setting

The network model and simulation parameters utilized for the simulation are presented in Table V. The test network comprises a Sink and eight sensing nodes, with the Sink located at the center of the torso. The initial positions of each node and the enhanced priorities are determined by the medical application type. The Sink and nodes are interconnected in a one-hop star topology. The requested allocation slot number is determined based on the effective payload size of the node application type. We conducted 100 simulations with a 95% confidence interval.

To establish a performance evaluation baseline, we selected four representative WBAN resource scheduling algorithms as benchmarks for comparison:

1) **IEEE 802.15.6 [11]**: As the standard protocol for WBANs, IEEE 802.15.6 defines a priority-based scheduling scheme that captures the heterogeneous characteristics of WBANs.
2) **CPMAC Algorithm [9]**: This algorithm employs a dynamic polling mechanism to balance energy efficiency and throughput.
3) **MCDM Algorithm [20]**: A scheduling approach based on the linear weighted sum method, it utilizes multiple cognitive metrics to adaptively adjust the scheduling order in response to changing network conditions.
4) **i-MAC Algorithm [31]**: This algorithm adopts a three-stage sorting and priority allocation protocol to effectively detect and handle critical events from sensors.

These algorithms were chosen because they are widely used to address key performance metrics such as latency, energy consumption, and throughput, which align closely with the metrics considered in our study. Furthermore, their mechanisms are well-suited for heterogeneous WBAN scenarios, ensuring a fair comparison. By comparing the proposed mechanism with these resource management algorithms, we aim to provide a comprehensive evaluation of its performance and applicability.

B. Average Delay

We utilize perceptual nodes to quantify the process of transmitting data to the receiving node in terms of average latency. Given that WBANs are deployed in short-distance environments, we omit relatively low propagation delays from the description. In Fig. 4(a), we present a comparison of latency and superframe count for personalized nodes under different priorities. When set to 200 superframes, we observe lower latency for high-priority nodes. This is due to the fact that in the initial phase, the algorithm prioritizes the transmission of data from high-priority nodes based on their personalized importance. Subsequently, after exceeding 200 superframes (400 superframes in total), priority 2 nodes are prioritized for transmission due to environmental changes, resulting in reduced latency. Within the next 200 superframes (600 total superframes), priority 3 nodes exhibit anomalous behavior. The skin activity detection node identifies priority 3 nodes as experiencing data anomalies due to emotional factors and continues real-time scheduling, consequently leading to sustained latency reduction for priority 2 nodes due to real-time environmental changes. Over the subsequent 200 superframes (800 superframes in total), priority 3 nodes are identified as having emergency data, triggering emergency transmission methods. Finally, within the last 200 superframes (a total of 1000 superframes), the system returns to real-time transmission status.

Meanwhile, to better illustrate the impact of different algorithms on the delay of heterogeneous nodes, we performed comparisons of the delay generated by different algorithms across different dimensions. In Fig. 4(b), we increased the superframe length to 1000 milliseconds for observation purposes. It was observed that as the superframe length increased, the delay generated by different algorithms did not show significant changes. This phenomenon is mainly due to the fact that nodes enter sleep mode after transmitting data, but our proposed algorithms still maintain lower latency.

As shown in Fig. 4(c) and Fig. 4(d), as the number of nodes or payload size changes, the delay generated by different algorithms increases. However, the delays produced by

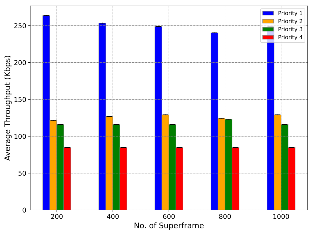

(a) Impact of varying no. of superframe.

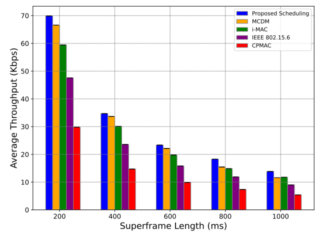

(b) Impact of varying superframe lengths.

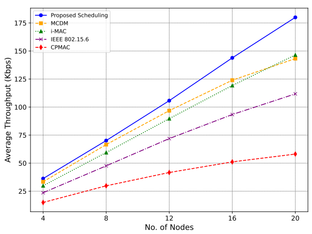

(c) Impact of varying no. of nodes.

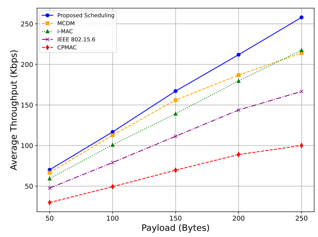

(d) Impact of varying payload.

Fig. 5. Comparison of average throughput.

these scheduling algorithms are all higher than those of our proposed algorithm. The reason for this is that our proposed scheduling algorithm prioritizes time slots for higher-priority nodes, thereby ensuring differentiated QoS for critical traffic and allowing scheduling adjustments based on changing environmental factors. In contrast, the traditional IEEE 802.15.6 protocol defines priorities but does not effectively account for real-time emergencies and environmental changes. The CP-MAC algorithm uses a round-robin approach, transmitting data to completion before moving on to the next data transmission. However, in the event of real-time environmental changes, it cannot guarantee the overall latency requirements, resulting in maximum delay. The i-MAC scheme uses an emergency quantity weighting method to determine the order, but does not consider real-time environmental changes. Although the MCDM algorithm considers real-time environmental changes and determines the final ranking scheme, it does not account for node heterogeneity.

C. Average Throughput

We define throughput as the process by which sensor nodes successfully transmit data packets to the sink node throughout the simulation time. In Fig. 5(a), we compare the throughput of personalized nodes under different priorities with the change in the number of superframes. When set to 200 superframes, we observe higher throughput for nodes with higher priority. This is because the algorithm takes into account the heterogeneity of the nodes, allowing nodes with higher priority to transmit more data. Subsequently, after 200 superframes (400 superframes in total), when real-time environmental changes occur, nodes with priority 2 are prioritized for transmission, resulting in increased throughput, while the throughput of nodes with priority 1 decreases. This is because the higher-priority nodes have more opportunities to successfully transmit packets after real-time sorting. For the next 200 superframes (600 superframes in total), priority 3 nodes experience abnormal conditions. Skin activity detection nodes determine that priority 3 nodes are experiencing data anomalies due to emotional factors and continue to use real-time scheduling. During this time, the throughput of priority 2 nodes continues to increase while the throughput of priority 1 nodes continues to decrease. In the next 200 superframes (800 superframes in total), nodes with priority 3 are treated as urgent data, which increases the chances of successful packet transmission for node 3. In the last 200 superframes (1000 superframes in total), the system returns to real-time transmission status.

Furthermore, to better reflect the impact of different algorithms on the throughput of heterogeneous nodes, we conducted comparisons of the throughput generated by different algorithms across various dimensions. Fig. 5(b) shows the superframe length increases, the throughput generated by different algorithms decreases. This is mainly due to the extension of the unit superframe time, yet our proposed algorithm still maintains higher throughput.

In Fig. 5(c) and Fig. 5(d), as the number of nodes increases or the payload size changes, the throughput generated by different algorithms increases. However, the throughput of these scheduling algorithms is lower than that of our proposed algorithm. Because our proposed scheduling algorithm takes into account the heterogeneity of nodes and ensures the transmission of physiological data packets in the best possible condition, adapting to changes in environmental factors. In contrast, traditional IEEE 802.15.6 protocol struggles to effectively handle packet loss caused by real-time changes in environmental factors. While the CPMAC algorithm prioritizes data packet transmission in favorable channel conditions, it fails to meet overall throughput requirements when environmental conditions fluctuate in real-time. Similarly, the i-MAC scheme, which prioritizes packets based on weighted urgency, cannot adequately respond to dynamic environmental changes. Although the MCDM algorithm considers real-time environmental changes and determines the final sorting scheme, its failure to prioritize urgent data packets results in lower overall throughput compared to our proposed algorithm.

D. Power consumption

We evaluate the average power consumption of nodes as the cumulative energy consumption of the idle, transmit, receive, and sleep states of the sensor node transceivers. In Fig. 6(a), we compared the power consumption of personalized nodes under different priorities by changing the number of superframes. At 200 superframes, we observed lower power consumption for higher priority nodes. This is due to the fact that the higher priority nodes transmit first, thus saving idle time. Subsequently, as the number of superframes exceeded 200 (400 superframes in total), environmental changes caused nodes with priority 2 to be prioritized for transmission, resulting in reduced idle delay and reduced power consumption, while nodes with priority 1 experienced increased idle delay and increased power consumption. For the next 200 superframes (600 superframes total), priority 3 nodes experienced abnormal conditions. Skin activity detection nodes determined

This article has been accepted for publication in a future issue of this journal, but has not been fully edited. Content may change prior to final publication.
Citation information: DOI: 10.1109/TCE.2025.3535142, IEEE Transactions on Consumer Electronics

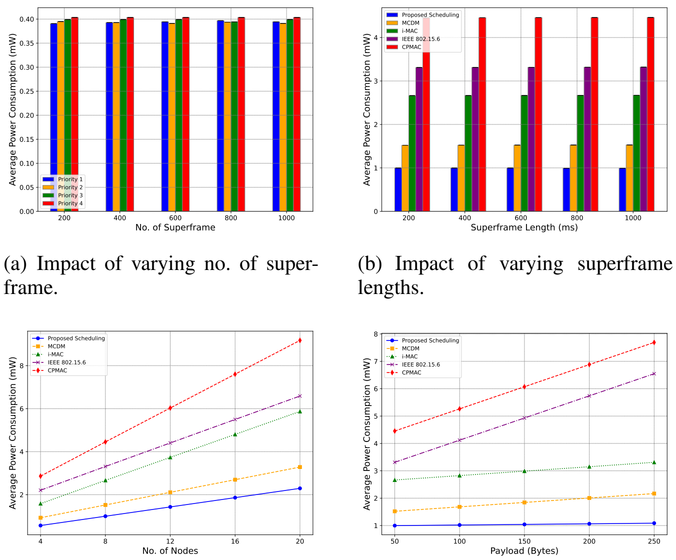

(a) Impact of varying no. of superframe.

(b) Impact of varying superframe lengths.

(c) Impact of varying no. of nodes.

(d) Impact of varying payload.

Fig. 6. Comparison of average power consumption.

that priority 3 nodes were experiencing data anomalies due to emotional factors and continued to use real-time scheduling, resulting in a sustained decrease in power consumption for priority 2 nodes. In the next 200 superframes (800 superframes in total), priority 3 nodes were identified as having urgent data and were transmitted urgently, resulting in a decrease in the average power consumption of priority 3 nodes. For the last 200 superframes (1000 superframes in total), the system returned to the real-time transmission state.

In addition, to better reflect the impact of different algorithms on the power consumption of heterogeneous nodes, we conducted multi-dimensional comparisons of the power consumption generated by different algorithms. In Fig. 6(b), with the increase in superframe length, the power consumption of nodes with different priorities slightly increases, mainly due to the slight increase in sleep state energy consumption. However, our proposed algorithm still maintains lower average power consumption.

Fig. 6(c) and Fig. 6(d) shows the number of nodes or the payload size changes, the power consumption generated by different algorithms also increases. Nevertheless, the power consumption of these scheduling algorithms is higher than that of our proposed algorithm. As the interpretation of the average delay in Fig. 4(c) and Fig. 4(d) suggests, the latency associated with idle, transmission, reception, and sleep states determines the average power consumption. Our proposed scheduling algorithm prioritizes time slots for nodes with higher priority and can adapt scheduling adjustments according to changes in environmental factors. In contrast, the traditional IEEE 802.15.6 protocol fails to effectively consider real-world emergencies and real-time changes in environmental factors. The CPMAC algorithm operates in a polling manner and cannot guarantee overall power consumption requirements in scenarios with real-time environmental changes. The i-MAC scheme does not account for real-time environmental changes. While the MCDM algorithm considers real-time environmental changes, it does not address the handling of urgent data packets.

E. Discussion

Compared to baseline algorithms, the proposed algorithm demonstrates significant advantages in terms of average delay, throughput, and power consumption. These results highlight the potential of our method for performance optimization, yet it is equally important to discuss the limitations of existing methods in real-world applications.

Firstly, as a standard protocol for WBANs, IEEE 802.15.6 defines node priorities to manage heterogeneous network demands. However, its simplified priority classification often fails to reflect the diversity and dynamics of real-world data requirements. This can result in inefficient transmission, especially in emergencies or under rapidly changing conditions. In contrast, our algorithm integrates personalized health features and environmental factors, enabling it to handle heterogeneity more effectively while reducing unnecessary communication overhead. It also introduces a personalized and adaptive scheduling mechanism to address the diverse demands of WBAN users.

Secondly, the CPMAC algorithm relies on a polling mechanism that performs well in stable environments but struggles under dynamic conditions. Our proposed method addresses this limitation by incorporating real-time environmental factors, such as node temperature and signal strength, into scheduling decisions, thereby enhancing reliability in variable environments.

Thirdly, while the MCDM algorithm prioritizes scheduling by adjusting indicator weights and focusing on nodes with higher link quality, it lacks robust mechanisms to manage urgent data uploads. Our approach introduces an enhanced weighted prioritization mechanism that not only addresses node heterogeneity but also ensures timely responses to critical data. For instance, integrating skin conductance nodes enables real-time anomaly detection, making it more suitable for dynamic scheduling scenarios.

Fourthly, the i-MAC scheme prioritizes tasks using urgency weighting but overlooks the impact of real-time environmental changes, which are crucial for scheduling efficiency. By continuously monitoring and adjusting priorities based on environmental factors, our algorithm ensures better adaptability to changing conditions, particularly in scenarios where environmental variability plays a key role.

While simulation results demonstrate the effectiveness of our proposed strategies, several practical challenges remain for real-world deployment. First, signal attenuation in varying environments may hinder the transmission of physiological data, potentially affecting scheduling decisions. Second, interference caused by interactions among body nodes or between individuals can lead to higher packet loss rates. Finally, variations in device configurations and materials may influence both user comfort and data accuracy. Addressing these challenges is essential to ensure the robustness and reliability of the proposed strategies in practical scenarios.

Remark 1. *We recognise the importance of ergonomic design and user experience for practical deployment, although this work focuses primarily on algorithmic design and performance evaluation of the proposed system. Future studies will address these aspects to ensure the system's usability and acceptance. Specific improvements will include: Developing lightweight, compact sensing nodes that minimize interference with daily activities. Exploring integration with existing wearable devices, such as smartwatches and fitness bands, to reduce the need for additional hardware components. Conducting usability studies across diverse user groups to assess long-term comfort and acceptance. Selecting flexible materials and optimizing node placement to enhance wearability and reduce obtrusiveness. These planned efforts aim to make the proposed system not only technically robust but also practically viable for widespread adoption.*

F. Relevance and Applications in CE

The proposed adaptive resource scheduling algorithm holds significant potential in addressing challenges in the CE industry, particularly in the context of wearable devices and smart home ecosystems. Below, we outline its relevance and potential applications:

1) **Challenges and Opportunities**: CE demand highly efficient and reliable systems to manage heterogeneous data and dynamic user environments. The proposed scheduling algorithm effectively addresses these demands by integrating personalized features and dynamic environmental adaptations. This ensures optimal performance under varying conditions, a key requirement in CE like smart-watches, fitness bands, and other wearable health monitoring devices. Furthermore, its emphasis on prioritizing emergency data ensures timely response, a critical feature in health-related devices.
2) **Potential Use Cases**: The algorithm has the potential to significantly enhance the performance of wearable devices, such as smart-watches and ECG monitors. By enabling real-time scheduling, it ensures the reliable transmission of health-critical data, including heart rate and blood pressure, while simultaneously optimizing energy efficiency. In addition, within a connected home environment, the algorithm can prioritize health monitoring data from multiple users, facilitating seamless integration with IoT devices to create a comprehensive health management ecosystem. Furthermore, its ability to classify emotional anomalies opens avenues for innovative CE applications, such as stress management systems and emotion-responsive interactive devices, thereby addressing both health and user experience dimensions in a unified framework.
3) **Benefits and Limitations**: The algorithm's reliance on accurate sensor data poses challenges in environments with significant interference. Furthermore, its integration with existing CE platforms may require additional compatibility adjustments, such as hardware-specific optimizations.

VII. Conclusion

This paper proposes an adaptive resource scheduling algorithm to address the resource allocation challenges in WBANs caused by node heterogeneity and environmental factors. Initially, a scheduling strategy is developed by incorporating both the heterogeneity of nodes and personalized requirements. Subsequently, nodes are prioritized based on real-time environmental characteristics to enhance resource utilization efficiency. Moreover, abnormal data are identified through emotional factors, and emergency data are prioritized for transmission to meet the performance demands of dynamic environments and urgent data delivery. The proposed algorithm not only effectively fulfills the performance requirements of high-priority nodes but also adapts to the dynamic and heterogeneous nature of WBANs. Simulation results demonstrate that the proposed approach outperforms existing algorithms in addressing performance requirements.

In addition, we will explore the application of the proposed algorithm in CE, particularly in wearable health monitoring devices and smart home systems. By integrating the algorithm with existing CE, such as fitness trackers and smart-watches, it can enhance user experience by delivering reliable real-time performance with minimal energy consumption. Future work will focus on constructing and validating a real-world WBAN test platform to further evaluate the performance of the proposed algorithm under practical conditions. This process will address key challenges such as signal attenuation, interference, and device variability, providing a comprehensive understanding of the algorithm's applicability and robustness in dynamic and heterogeneous WBAN environments. Furthermore, future research will prioritize experimental validation of the system's ergonomic design, emphasizing user comfort, device integration, and usability across diverse scenarios. These efforts aim to ensure the system's readiness for practical deployment and alignment with real-world user requirements.

References

[1] C. K. Wu, C.-T. Cheng, Y. Uwate, G. Chen, S. Mumtaz, and K. F. Tsang, "State-of-the-art and research opportunities for next-generation consumer electronics," *IEEE Trans. Consum. Electron.*, vol. 69, no. 4, pp. 937–948, Nov. 2023.

[2] E. El-Adawi, E. Essa, M. Handosa, and S. Elmougy, "Wireless body area sensor networks based human activity recognition using deep learning," *Sci. Rep.*, vol. 14, no. 1, p. 2702, Feb. 2024.

[3] M. Shahid, M. Tariq, Z. Iqbal, H. M. Albarakati, N. Fatima, M. A. Khan, and M. Shabaz, "Link-quality-based energy-efficient routing protocol for WSN in IoT," *IEEE Trans. Consum. Electron.*, vol. 70, no. 1, pp. 4645–4653, Feb. 2024.

[4] S. P. Mohanty and F. Pescador, "Introduction consumer technologies for smart healthcare," *IEEE Trans. Consum. Electron.*, vol. 67, no. 1, pp. 1–2, Feb. 2021.

[5] D. Fernandes, A. G. Ferreira, R. Abrishambaf, J. Mendes, and J. Cabral, "Survey and taxonomy of transmissions power control mechanisms for wireless body area networks," *IEEE Commun. Surv. Tutor.*, vol. 20, no. 2, pp. 1292–1328, Dec. 2018.

[6] G. Mehmood, M. Z. Khan, A. Waheed, M. Zareei, and E. M. Mohamed, "A trust-based energy-efficient and reliable communication scheme (trust-based ERCS) for remote patient monitoring in wireless body area networks," *IEEE Access*, vol. 8, pp. 131 397–131 413, Jul. 2020.

[7] J.-H. Syu, J. C.-W. Lin, G. Srivastava, and K. Yu, "A comprehensive survey on artificial intelligence empowered edge computing on consumer electronics," *IEEE Trans. Consum. Electron.*, vol. 69, no. 4, pp. 1023–1034, Sep. 2023.

[8] S. Pattanaik, C. Chakraborty, S. Behera, S. K. Majhi, and S. K. Pani, “An MIoT framework of consumer technology for medical diseases prediction,” *IEEE Trans. Consum. Electron.*, vol. 70, no. 1, pp. 3754–3761, Mar. 2024.

[9] C.-H. Lin, K. C.-J. Lin, and W.-T. Chen, “Channel-aware polling-based MAC protocol for body area networks: Design and analysis,” *IEEE Sensors J.*, vol. 17, no. 9, pp. 2936–2948, Feb. 2017.

[10] G. Mehmood, M. Z. Khan, A. K. Bashir, Y. D. Al-Otaibi, and S. Khan, “An efficient QoS-based multi-path routing scheme for smart healthcare monitoring in wireless body area networks,” *Comput. Electr. Eng.*, vol. 109, p. 108517, Jul. 2023.

[11] S. Movassaghi, M. Abolhasan, J. Lipman, D. Smith, and A. Jamalipour, “Wireless body area networks: A survey,” *IEEE Commun. Surv. Tutor.*, vol. 16, no. 3, pp. 1658–1686, Jan. 2014.

[12] G. Sun, K. Wang, H. Yu, X. Du, and M. Guizani, “Priority-based medium access control for wireless body area networks with high-performance design,” *IEEE Internet Things J.*, vol. 6, no. 3, pp. 5363–5375, Feb. 2019.

[13] Z. Ning, P. Dong, X. Wang, X. Hu, L. Guo, B. Hu, Y. Guo, T. Qiu, and R. Y. K. Kwok, “Mobile edge computing enabled 5G health monitoring for internet of medical things: A decentralized game theoretic approach,” *IEEE J. Select. Areas Commun.*, vol. 39, no. 2, pp. 463–478, Feb. 2021.

[14] K. Das, S. Moulik, and C.-Y. Chang, “Priority-based dedicated slot allocation with dynamic superframe structure in IEEE 802.15.6-based wireless body area networks,” *IEEE Internet Things J.*, vol. 9, no. 6, pp. 4497–4506, Aug. 2022.

[15] D. Wu, B. Yang, H. Wang, D. Wu, and R. Wang, “An energy-efficient data forwarding strategy for heterogeneous WBANs,” *IEEE Access*, vol. 4, pp. 7251–7261, Sep. 2016.

[16] Z. Liu, B. Liu, and C. W. Chen, “Buffer-aware resource allocation scheme with energy efficiency and QoS effectiveness in wireless body area networks,” *IEEE Access*, vol. 5, pp. 20 763–20 776, Oct. 2017.

[17] B. Liu, Z. Yan, and C. W. Chen, “Medium access control for wireless body area networks with QoS provisioning and energy efficient design,” *IEEE Trans. Mobile Comput.*, vol. 16, no. 2, pp. 422–434, Mar. 2017.

[18] Z. Ullah, I. Ahmed, F. A. Khan, M. Asif, M. Nawaz, T. Ali, M. Khalid, and F. Niaz, “Energy-efficient harvested-aware clustering and cooperative routing protocol for WBAN (E-HARP),” *IEEE Access*, vol. 7, pp. 100 036–100 050, Jul. 2019.

[19] B. Liang, M. S. Obaidat, X. Liu, H. Zhou, and M. Dong, “Resource scheduling based on priority ladders for multiple performance requirements in wireless body area networks,” *IEEE Trans. Veh. Technol.*, vol. 70, no. 7, pp. 7027–7036, Jul. 2021.

[20] B.-S. Kim and K.-I. Kim, “A priority-based dynamic link scheduling algorithm using multi-criteria decision making in wireless body area networks,” in *Proc. IEEE 28th Int. Conf. (MASCOTS), Nice, France*, Nov. 2020, pp. 1–8.

[21] S. Misra and S. Sarkar, “Priority-based time-slot allocation in wireless body area networks during medical emergency situations: An evolutionary game-theoretic perspective,” *IEEE J. Biomed. Health Informat.*, vol. 19, no. 2, pp. 541–548, Mar. 2015.

[22] D.-R. Chen and W.-M. Chiu, “Collaborative link-aware protocols for energy-efficient and QoS wireless body area networks using integrated sensors,” *IEEE Internet Things J.*, vol. 5, no. 1, pp. 132–149, Feb. 2018.

[23] A. Samanta, S. Bera, and S. Misra, “Link-quality-aware resource allocation with load balance in wireless body area networks,” *IEEE Syst. J.*, vol. 12, no. 1, pp. 74–81, Mar. 2018.

[24] Z. Liu, B. Liu, and C. W. Chen, “Transmission-rate-adaption assisted energy-efficient resource allocation with QoS support in WBANs,” *IEEE Sensors J.*, vol. 17, no. 17, pp. 5767–5780, Sep. 2017.

[25] J. Ramis-Bibiloni and L. Carrasco-Martorell, “Energy-efficient and QoS-aware link adaptation with resource allocation for periodical monitoring traffic in SmartBANs,” *IEEE Access*, vol. 8, pp. 13 476–13 488, Jan. 2020.

[26] E. Selem, M. Fatehy, and S. M. A. El-Kader, “mobTHE (mobile temperature heterogeneity energy) aware routing protocol for WBAN IoT health application,” *IEEE Access*, vol. 9, pp. 18 692–18 705, Jan. 2021.

[27] Z. Mao, F. Hu, Z. Li, Z. Ling, and S. Li, “Energy-efficient optimization in multi-sensor WBAN with multi-antenna AP,” *IEEE Access*, vol. 7, pp. 115 409–115 417, Jul. 2019.

[28] L. Zhang, P. Lin, K. Deng, G. Huang, and J. Feng, “Joint optimization of energy and QoS for smart clothing with multiposture participation,” *IEEE Sensors J.*, vol. 22, no. 23, pp. 23 529–23 538, Dec. 2022.

[29] D. Fernandes, A. G. Ferreira, R. Abrishambaf, J. Mendes, and J. Cabral, “A low traffic overhead transmission power control for wireless body area networks,” *IEEE Sensors J.*, vol. 18, no. 3, pp. 1301–1313, Feb. 2018.

[30] S. Memon, J. Wang, A. R. Bhangwar, S. M. Fati, A. Rehman, T. Xu, and L. Zhang, “Temperature and reliability-aware routing protocol for wireless body area networks,” *IEEE Access*, vol. 9, pp. 140 413–140 423, Oct. 2021.

[31] S. Misra, P. K. Bishoyi, and S. Sarkar, “i-MAC: In-body sensor MAC in wireless body area networks for healthcare IoT,” *IEEE Syst. J.*, vol. 15, no. 3, pp. 4413–4420, Sep. 2021.

[32] B. Liang, X. Liu, H. Zhou, V. C. M. Leung, A. Liu, and K. Chi, “Channel resource scheduling for stringent demand of emergency data transmission in WBANs,” *IEEE Trans. Wireless Commun.*, vol. 20, no. 4, pp. 2341–2352, Apr. 2021.

[33] Y.-H. Xu, L. Suo, W. Zhou, and G. Yu, “A graph-learning-inspired resource optimization for digital-twin-empowered wireless body area networks,” *IEEE Sens. Lett.*, vol. 7, no. 11, pp. 1–4, Nov. 2023.

[34] K. S. Deepak and A. V. Babu, “Improving reliability of emergency data frame transmission in IEEE 802.15.6 wireless body area networks,” *IEEE Syst. J.*, vol. 12, no. 3, pp. 2082–2093, Sep. 2018.

[35] D. D. Olatinwo, A. M. Abu-Mahfouz, G. P. Hancke, and H. C. Myburgh, “Energy efficient priority-based hybrid MAC protocol for IoT-enabled WBAN systems,” *IEEE Sensors J.*, vol. 23, no. 12, pp. 13 524–13 538, Jun. 2023.

[36] D. D. Olatinwo, A. M. Abu-Mahfouz, and Z. Hancke, “Energy-efficient multichannel hybrid MAC protocol for IoT-enabled WBAN systems,” *IEEE Sensors J.*, vol. 23, no. 22, pp. 27 967–27 983, Nov. 2023.

[37] A. Manirabona, S. Boudjit, and L. C. Fourati, “A priority-weighted round robin scheduling strategy for a WBAN based healthcare monitoring system,” in *Proc. IEEE 13th Int. Conf. Annual Consumer Commun. Netw. Conf. (CCNC), Las Vegas, USA, Jan.*, 2016, pp. 224–229.

[38] S. Misra, S. Moulik, and H.-C. Chao, “A cooperative bargaining solution for priority-based data-rate tuning in a wireless body area network,” *IEEE Trans. Wireless Commun.*, vol. 14, no. 5, pp. 2769–2777, May 2015.

[39] S. Moulik, S. Misra, and D. Das, “AT-MAC: Adaptive MAC-frame payload tuning for reliable communication in wireless body area networks,” *IEEE Trans. Mobile Comput.*, vol. 16, no. 6, pp. 1516–1529, Jun. 2017.

[40] B.-S. Kim, B. Shah, and K.-I. Kim, “Adaptive scheduling and power control for multi-objective optimization in IEEE 802.15.6 based personalized wireless body area networks,” *IEEE Trans. Mobile Comput.*, vol. 22, no. 11, pp. 6251–6268, Nov. 2023.

[41] D. Yang, M. C. Converse, D. M. Mahvi, and J. G. Webster, “Expanding the bioheat equation to include tissue internal water evaporation during heating,” *IEEE Trans. Biomed. Eng.*, vol. 54, no. 8, pp. 1382–1388, Aug. 2007.

[42] A. Arthur, A. Takahiro, C. Chihong, and K. Sung-Weon, “Channel models WBAN-holst centre/ IMEC-NL,” *IEEE Standard 802.15–08–0418-01-0006*, 2009.

Zheng Zhang (Member, IEEE) received the M.S. degree in Electronics and Communications Engineering from Chongqing University of Posts and Telecommunications, Chongqing, China, in 2015. He is currently pursuing a Ph.D. degree in Communication and Information Engineering at the same institution while serving as a Visiting Ph.D. Scholar at Brunel University of London, UK. His research interests include WBANs, smart healthcare, wearable devices, and human-computer interaction.

Citation information: DOI: 10.1109/TCE.2025.3535142, IEEE Transactions on Consumer Electronics

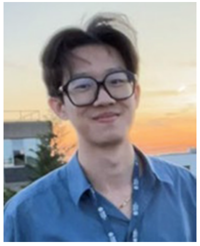

Xinxing Ren (Student Member, IEEE) received the B.Eng. degree (with First-Class Hons.) in electronic and electrical engineering from the Brunel University of London, Uxbridge, U.K., in 2022, where he is currently pursuing the Ph.D. degree. He is a member of the Brunel Interdisciplinary Power Systems Research Centre, Brunel University of London. His research interests include connected vehicles, wireless body area networks, and embodied intelligence.

Chun Sing Lai (Senior Member, IEEE) received the B.Eng. (First Class Hons.) in electronic and electrical engineering from Brunel University of London, UK, in 2013, and the D.Phil. degree in engineering science from the University of Oxford, UK, in 2019. He is currently a Senior Lecturer with the Department of Electronic and Electrical Engineering and Course Director of MSc Electric Vehicle Systems at Brunel University of London. His research interests are in power system optimization and electric vehicle systems. Dr. Lai was a Technical Program Co-Chair for 2022 IEEE International Smart Cities Conference. He is the Vice-Chair of the IEEE Smart Cities Publications Committee. He is an Associate Editor for IEEE Transactions on Systems, Man, and Cybernetics: Systems, IEEE Transactions on Consumer Electronics and IET Energy Conversion and Economics. He is the Working Group Chair for IEEE P2814 and P3166 Standards, an Associate Vice President, Systems Science and Engineering of the IEEE Systems, Man, and Cybernetics Society (IEEE/SMCS) and Co-Chair of the IEEE SMC Intelligent Power and Energy Systems Technical Committee. He is a recipient of the 2022 Meritorious Service Award from the IEEE SMC Society for ”meritorious and significant service to IEEE SMC Society technical activities and standards development”. He is an IET Member, Chartered Engineer, and Fellow of the Higher Education Academy.

Ruiheng Wu (Senior Member, IEEE) received his BEng and MEng degrees from Tianjin University, China, in 1982 and 1986 respectively. Following 10 years as a faculty member in the Department of Electronic Engineering at Tianjin University and two years research at the City University of Hong Kong, he joined the Analogue Circuit Design Research Group at Oxford Brookes University, U.K., as a PhD student in January 1999, where he completed his PhD thesis entitled ’Design of Wide Bandwidth High Linearity Amplifiers’. Currently, Dr Wu is a senior lecturer in Electronic and Electrical Engineering at Brunel University London. Dr Wu’s general research interests are in the area of analogue signal processing and integrated circuit design; RF circuits and systems; remote health monitoring and applications of modern electronics in life search and rescue. In recent years, as a principal investigator, he has been involved in many industrial and research projects supported by EU, NHS, HEFCE etc. and has several tens publications in his research areas.

Jinzhao Lin received the master’s and Ph.D. degrees from Chongqing University, Chongqing, China, in 1995 and 2001, respectively. He is currently a Professor with the School of Communication and Information Engineering, Chongqing University of Posts and Telecommunications, Chongqing. His main research interests include theoretical, technical, methodological, and applied research on smart medical devices and their intersections.

Zhangyong Li received the Ph.D. degree from Chongqing Medical University, Chongqing, China, in 2004. He is currently a Professor with the School of Bioinformatics, Chongqing University of Posts and Telecommunications, Chongqing. His main research interests include biomedical information processing, digital medical instrument design, electromagnetic radiation protection technology, environmental assessment, and reliability of medical instruments.